Talanta 85 (2011) 2411–2416

Contents lists available at ScienceDirect

Talanta

journal homepage: www.elsevier.com/locate/talanta

Highly sensitive hydrazine chemical sensor based on mono-dispersed rapidly synthesized PEG-coated ZnS nanoparticles

Surinder K. Mehta [a,*], Khushboo [a], Ahmad Umar [b]

[a] Department of Chemistry and Centre of Advanced Studies in Chemistry, Panjab University, Chandigarh 160 014, India
[b] Collaborative Research Centre for Sensors and Electronic Devices (CRCSED), Centre for Advanced Materials and Nano-Engineering (CAMNE), Najran University, PO Box 1988, Najran 11001, Saudi Arabia

ARTICLE INFO

Article history:
Received 30 June 2011
Accepted 25 July 2011
Available online 24 August 2011

Keywords:
PEG-coated ZnS nanoparticles
Hydrazine
Chemical sensor
Amperometry

ABSTRACT

Monodispersed PEG-coated ZnS (P-ZnS) nanoparticles (NPs) were synthesized by facile microwave process and utilized as efficient electron mediators for the fabrication of highly sensitive hydrazine chemical sensor. The detailed morphological and structural properties revealed the monodispersity and good crystallinity for synthesized P-ZnS NPs. A high-sensitivity of ~89.3 μA cm^{-2} μM and low limit of detection of 1.07 μM, based on S/N ratio, were obtained for the fabrication of hydrazine chemical sensor based on P-ZnS NPs. To the best of our knowledge, this is the first report which demonstrates the utilization of P-ZnS NPs for the fabrication of efficient hydrazine chemical sensor. By this work, it could be concluded that simply synthesized ZnS NPs can be used as efficient electron mediators for the fabrication of effective hydrazine chemical sensors.

1. Introduction

With recent advances in nanotechnology, nanoparticles (NPs) based electrochemical detection of hazardous compounds has drawn a considerable attention from scientists as the unique properties of NPs result into a very high sensitivity. In this regard, many achievements have been made in the field of amperometric and voltammetric electrochemical sensors [1–3]. Among various electrochemical sensors, the hydrazine sensors have gained considerable attention because of its large applicability and high toxicity. Hydrazine possesses many practical applications in various fields, to name a few, pharmaceutical intermediates, photographic chemicals, corrosion protection treatments for boilers, rocket propellants, pesticides, fuel cells, etc. [4]. In spite of its numerous advantages, hydrazine is neurotoxin in nature and has been classified as human carcinogen by Environmental Protection Agency (EPA). The toxic nature of hydrazine limits its applications; hence there is a real need of highly sensitive, simple and economic methods for determination of hydrazine. Various methods for the detection of hydrazine have been reported in the literature which includes chemiluminescence [5], spectrophotometry [6], coulometric titration [7], and so on. However, the electrochemical sensing methods possess a special place and are of particular interest due to their simplicity and low-cost fabrication process.

Among various II–VI semiconductor nanostructured materials, zinc sulphide (ZnS) possesses a special place due to its useful properties and wide applications [1]. The properties of ZnS include its wide band gap (3.7 eV) at room-temperature, relatively large exciton binding energy (~40 meV), high index of refraction and a high transmittance in the visible range and so on [1,8–11]. Due to many useful properties, ZnS NPs are widely used in electroluminescence, non-linear optical devices, light emitting diodes, applications in flat-panel displays, electroluminescence devices, photonic crystal devices, lasers, photocatalysis, etc. [1,12–14]. Even though ZnS NPs possess various excellent properties and used in variety of high-efficient technological applications but yet have not been used for electrochemical sensor applications.

In this article, a facile and very rapid method has been introduced for the synthesis of monodisperse polyethylene glycol (PEG-2000) coated ZnS (P-ZnS) NPs. It is known that due to the high surface area, the nanoparticles surface has to be functionalized with suitable ligands to make them stable. These ligands prevent aggregation and precipitation of nanoparticles. In this regard, the biocompatible polymers like PEG offer a good choice of ligands to stabilize nanoparticles. The prepared P-ZnS NPs have been characterized in detail in terms of their structural and optical properties and efficiently utilized as effective electron mediators for the fabrication of highly sensitive hydrazine chemical sensor. The fabricated hydrazine sensor based on P-ZnS NPs exhibits a good electrocatalytic activity towards electrochemical oxidation of hydrazine. A very high sensitivity and low detection limit have been achieved from the fabricated hydrazine sensor. To the best of our knowledge, this is the first report in which P-ZnS NPs modified Au electrode

* Corresponding author. Tel.: +91 172 2534423; fax: +91 172 2545074.
E-mail addresses: skmehta@pu.ac.in (S.K. Mehta), ahmadumar786@gmail.com (A. Umar).

0039-9140/$ – see front matter © 2011 Elsevier B.V. All rights reserved.
doi:10.1016/j.talanta.2011.07.089

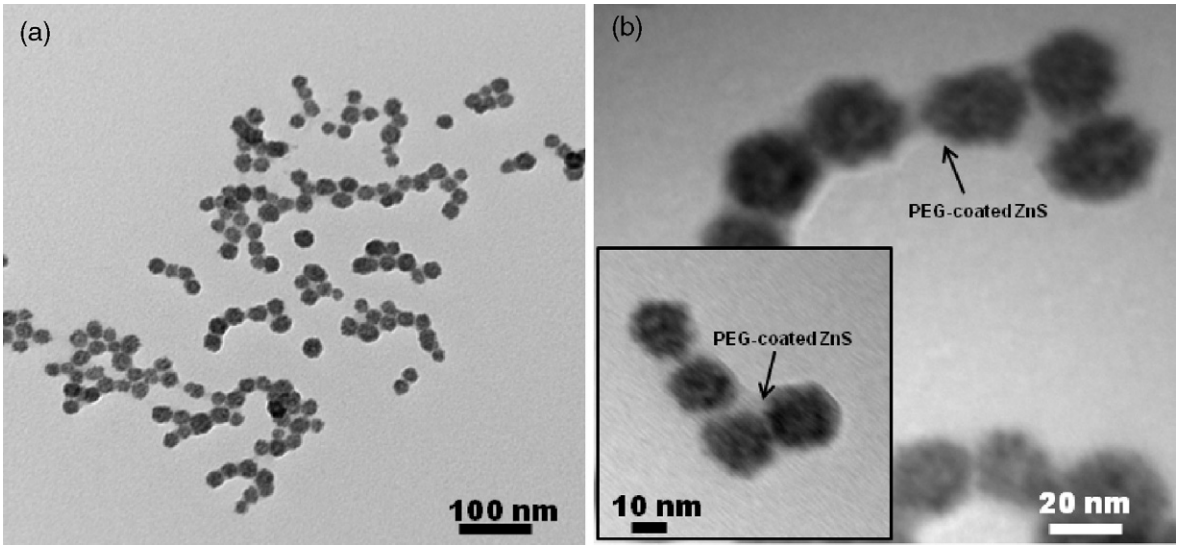

Fig. 1. Typical TEM images of as-synthesized PEG coated ZnS nanoparticles prepared by microwave process.

has been used for the fabrication of amperometric hydrazine sensor.

2. Materials and methods

2.1. Materials

PEG-2000 was purchased from Fluka Chemika. Zinc acetate ($Zn(CH_3COO)_2{\cdot}2H_2O$) (ZOAc) and thioacetamide (CH_3CSNH_2) (TA) were obtained from CDH, India. All the chemicals were used as received without further purification. Deionized water (DW) was used for all the experiments.

2.2. Synthesis and characterization of PEG-coated ZnS nanoparticles

P-ZnS NPs were synthesized by facile microwave process by using ZOAc, TA and PEG-2000. In a typical reaction process, 10 mM of PEG was dissolved in 10 ml DW. Consequently, 0.005 M ZOAc solution made in 10 ml DW and 0.005 M TA solution prepared in 10 ml DW were added in the prepared PEG solution. The final solution was then placed in a domestic microwave (MW; IFB-20PG2S) oven at optimized reaction conditions, i.e. 60% power for 20 s. The optimized provided power supply was 230 V/50 Hz, consumption was 1200 W, output power was 800 W and operation frequency was 2450 MHz. After completing the reaction, the solution was cooled at room-temperature and the obtained ZnS NPs were characterized in detail in terms of their morphological, structural and optical properties. The NPs were also used as efficient electron mediators to fabricate hydrazine amperometric chemical sensor.

The morphological investigation of as-synthesized NPs was done by transmission electron microscopy (TEM) at 80 kV (Hitachi H-7500) while the structural characterization was done by X-ray diffractometer (XRD; PANalytical X'Pert PRO) measured with Cu-Kα radiations (λ = 1.54178 Å) in the range of 10–70° with scan speed of 8°/min. To check the particle size distribution, particle size analysis (PSA) was performed using Malvern Zetasizer nanoseries. To examine the optical properties of P-ZnS NPs, room-temperature UV–Vis spectrum (Thermo Fisher Scientific Evolution 160 UV–Vis spectrophotometer) was recorded.

2.3. Fabrication of hydrazine chemical sensor based on PEG-coated ZnS nanoparticles

To fabricate the hydrazine chemical sensor, the P-ZnS NPs were coated on the surface of gold electrode (Au; surface area = 3.14 mm^2) which acts as a working electrode to evaluate the sensor performance. Prior to use, the Au electrode was polished with alumina slurry, sonicated in distilled water and dried at room-temperature. Slurry of P-ZnS NPs was made by using butyl carbitol acetate (BCA) and coated on the surface of Au electrode to modify it. The modified Au electrode was then dried at 60 ± 5 °C for 4–6 h to get a uniform and dry layer over entire electrode surface.

All electrochemical experiments have been performed at room-temperature with a μAutolab Type-III cyclic voltammeter using three-electrode configuration. For all the electrochemical measurements, P-ZnS NPs modified Au electrode was used as working electrode, a Pt wire as a counter electrode and an Ag/AgCl (sat. KCl) as a reference electrode. For all the measurements, 0.1 M phosphate buffer solution (PBS; pH 7.0) was used.

3. Results and discussion

3.1. Morphological, structural and optical properties of PEG-coated ZnS nanoparticles

The general morphologies of P-ZnS products have been characterized by transmission electron microscopy (TEM) and results are presented in Fig. 1. For TEM measurement, a drop of aqueous solution of NPs was placed on a copper grid and examined. Fig. 1(a) exhibits the typical low-resolution TEM image which confirms the general morphology of NPs. It is clear from the micrograph that the as-synthesized NPs are monodispersed with spherical in shape. Most of the nanoparticles possess almost similar diameter, however, few less diameter nanoparticles are also seen in the micrograph. The typical diameters of the nanoparticles are in the range of 11 ± 3 nm. Fig. 1(b) exhibits the typical high-resolution TEM images of NPs. It is clear from the micrograph that a very thin layer of PEG is uniformly coated on the surface of the synthesized nanoparticles (inset 1 (b)).

To examine the crystallinity and crystal phases of as-synthesized P-ZnS NPs, X-ray diffraction has been done and the results are presented in Fig. 2(a). Three well defined diffraction

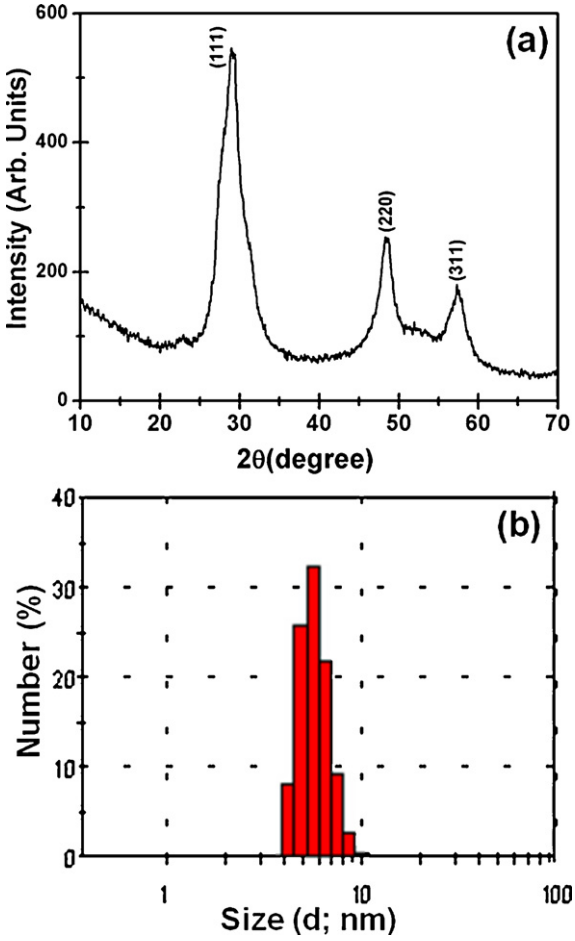

Fig. 2. Typical (a) X-ray diffraction pattern and (b) particle size distribution obtained from particle size analyzer of as-synthesized PEG coated ZnS nanoparticles.

peaks have been observed in the obtained XRD pattern. The diffraction peaks appeared at $2\theta = 29^\circ$, 48.4° and 57.4° which correspond to (1 1 1), (2 2 0), and (3 1 1) lattice plane, respectively. This confirms the cubic zinc blende structure of prepared P-ZnS NPs. In the obtained pattern, no characteristic peak related with any impurity has been observed, within the resolution limit of the XED diffractometer which shows the pure phase formation of prepared ZnS NPs. In addition to this, the broadening in the diffraction peaks depicts that the synthesized product is in nanoscale. The particle size distribution of as-synthesized P-ZnS NPs has been characterized by particle size analyzer (PSA). Fig. 2(b) shows the typical particle size distribution graph which reveals that the average diameter of synthesized P-ZnS NPs is ~7 nm. The polydispersity index (PDI) of synthesized nanoparticles is found to be 0.19 that confirms the monodispersity of synthesized NPs.

To examine the optical properties of synthesized P-ZnS NPs, UV–Vis spectrum was recorded at room-temperature. For UV–Vis measurements, the synthesized products were ultrasonically dispersed in water and 1 ml of this solution was used for analysis. PEG was taken as a reference. Fig. 3 depicts typical UV–Vis spectrum of synthesized P-ZnS NPs that shows a well-defined absorption peak at 293 nm. It is well known that the relationship between absorption coefficient and the incident photon energy of semiconductors can be obtained by using Tauc's formula (Eq. (1)).

$$(\alpha h\nu) = A(h\nu - E_g)^n \quad (1)$$

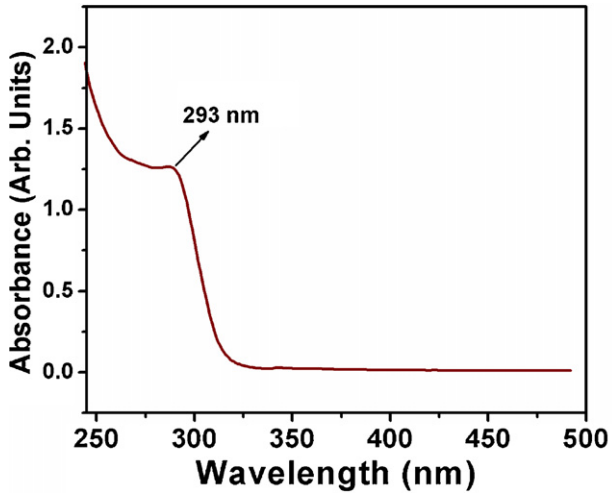

Fig. 3. Typical UV–Vis spectrum of as-synthesized PEG coated ZnS nanoparticles prepared by facile microwave process.

where α is the absorption coefficient, A is constant, and n is equal to ½ for a direct transition semiconductor and 2 for indirect transition semiconductor. Therefore, by considering the Tauc's equation, the optical band gap (E_g) can be experimentally obtained from absorption coefficient. The calculated optical band gap for the synthesized P-ZnS NPs is 4.23 eV, which is considerably higher and blue shifted from the bulk zinc blende ZnS with optical band gap of 3.65 eV. This phenomenon may be due to the quantum size effect of the synthesized structures with the appearance of blue shift.

The growth of P-ZnS NPs can be well understood based on the chemical reactions involved in the synthesis process. During the reaction, ZOAc dissociates into zinc ions (Zn^{2+}) and acetate (Ac) ions. Similarly, the fast heating in microwave process in the presence of PEG accelerates the decomposition of thioacetamide to provide S^{2-} ions. This phenomenon can be understood through a simple chemical reaction mentioned below:

$$CH_3CSNH_2 + H_2O \xrightarrow{MW} CH_3CONH_2 + H_2S$$

$$H_2S \rightarrow 2H^+ + S^{2-}$$

The nucleation of ZnS occurs due to the reaction between Zn^{2+} and S^{2-} ions according to the chemical reaction mentioned below:

$$Zn^{+2} + S^{2-} \rightarrow ZnS$$

The initially formed ZnS nuclei act as building blocks for the formation of final product. With time under proper reaction conditions, the concentration of ZnS nuclei increases which leads the formation of final products.

During the reaction, PEG gets adsorbed on the surface of ZnS NPs with their hydrophilic –OH groups spread out into water. Fig. 4 illustrates a typical stabilization structure of ZnS NPs by PEG in aqueous solution. Therefore, as a final product, P-ZnS NPs were obtained under the reaction conditions employed.

3.2. *Electrochemical hydrazine chemical sensor performance of P-ZnS NPs modified gold electrodes*

For the fabrication of hydrazine chemical sensor, the synthesized P-ZnS NPs were used as supporting mediator for the modification of Au electrode The modified electrode was used as a working electrode to determine the electrochemical activity towards hydrazine oxidation using cyclic voltammetry. The cyclic

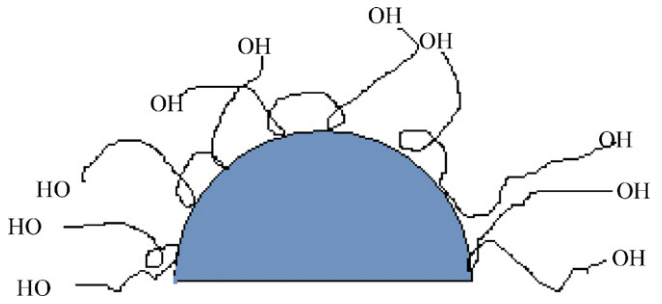

Fig. 4. Schematic presentation of stabilizing structure of PEG coating on surface of ZnS NPs.

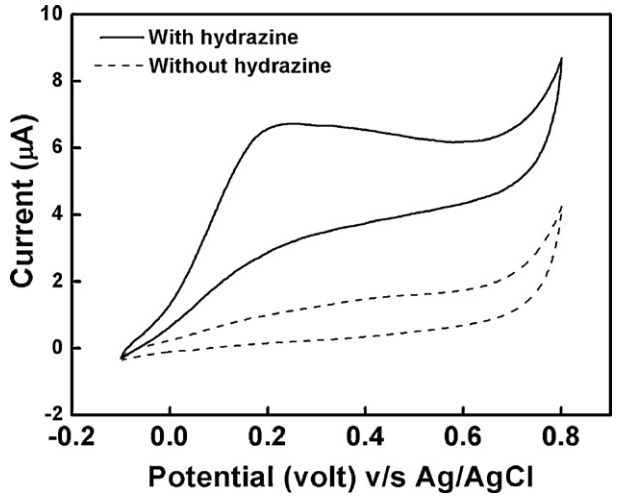

Fig. 5. Cyclic voltammetric sweep curve for the P-ZnS NPs/Au electrode without hydrazine (dashed line) and with 1 mM hydrazine (solid line) in 0.1 M PBS (pH 7.0). The scan rate was 50 mV s^{-1}.

voltammograms (CV) of the hydrazine using P-ZnS NPs modified gold (P-ZnS/Au) electrode in a 0.1 M phosphate buffer solution (PBS) (pH 7.0) with 1 mM hydrazine (solid line) and without hydrazine (dotted line), at a scan rate of 50 mV s^{-1}, are shown in Fig. 5.

It is apparent from the obtained CV graph that in the absence of hydrazine, the P-ZnS NPs modified Au electrode does not show any redox peak in the potential range of −0.1 to 0.8 V. However, on the other hand, when used in the presence of hydrazine at the same experimental conditions and setup, a significant enhancement in anodic peak at potential +0.21 V and current 6.9 μA have been observed. The electrochemical response of hydrazine is irreversible as no cathodic current is observed in the reverse sweep. These observations conclude that the synthesized P-ZnS NPs are effective mediator for efficient detection of hydrazine.

To check the effect of scan rates, the cyclic voltammograms of P-ZnS NPs modified Au electrode was examined at various scan rates, from 50 mV s^{-1} to 800 mV s^{-1}, in 0.1 M PBS buffer solution (pH 7.0), containing 1 mM hydrazine. Fig. 6(a) shows typical CV responses of P-ZnS NPs modified Au electrode at various scan rates. It is clear that with increasing the scan rates, the peak current is also increasing. Interestingly, at different scan rates, slight shifts in the anodic peak potentials were also observed in the range of +0.21 to +0.32 V. Fig. 6(b) depicts a plot for the anodic (I_a) peak currents versus the square root of the scan rates ($\nu^{1/2}$). The anodic peak current exhibits a linear dependence with square root of scan rates. The number of electrons involved in overall reaction (n) can be calculated from Randles–Sevcik equation (Eq. (2))

$$ip = (2.69 \times 10^5) n^{3/2} A D^{1/2} \nu^{1/2} C \quad (2)$$

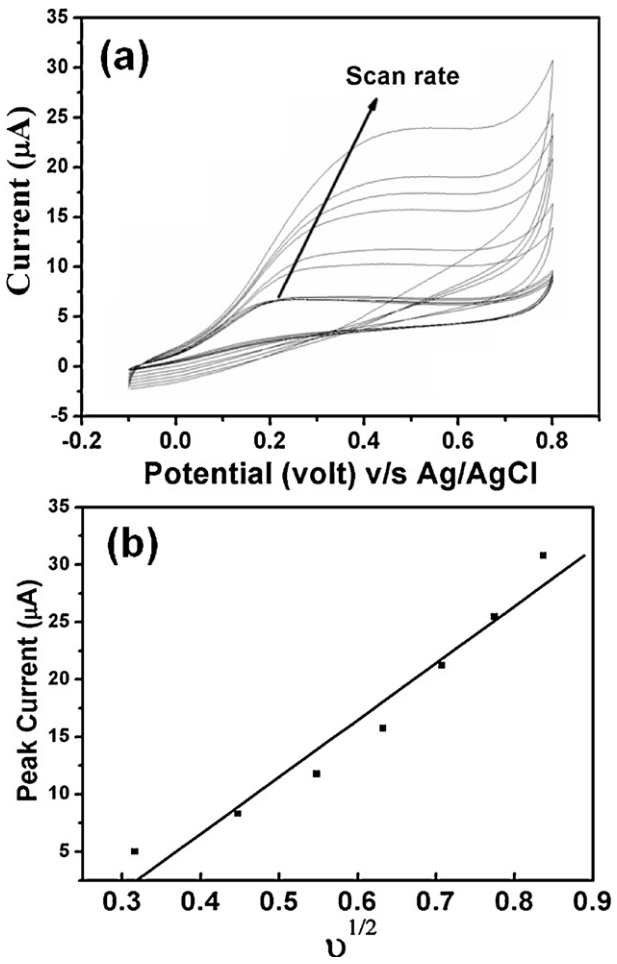

Fig. 6. (a) Cyclic voltammograms obtained for P-ZnS NPs/Au electrode in 0.1 M PBS containing 1 mM hydrazine at various scan rates from 50 mV s^{-1} to 800 mV s^{-1}. (b) Plot for the anodic peak current versus the square root of the scan rates ($\nu^{1/2}$) in same solution.

where n is the number of electron equivalent exchanged during the redox process, A (cm^2) is the active area of the working electrode, D (cm^2 s^{-1}) and C (mol cm^{-3}) are the diffusion coefficient and the bulk concentration of hydrazine and ν is the voltage scan rate (V s^{-1}). The total number of electrons involved in oxidation is estimated to be 2. Thus the mechanism for oxidation of hydrazine at ZnS/Au electrode can be proposed as [15].

$$N_2H_4 + 5/2OH^- \rightarrow 1/2N^-{}_3 + 1/2NH_3 + 5/2H_2O + 2e^-$$

To investigate, in detail, the sensor performance of P-ZnS NPs modified Au electrode, amperometry experiments have been carried out under stirred conditions. The results are demonstrated in Fig. 7. The stirring condition could enhance the current sensitivity in the amperometric experiments. Fig. 7(a) gives the typical amperometric response of the P-ZnS NPs modified electrode on a successive addition of hydrazine from 0.1 μM to 1 μM at constant potential in 0.1 M PBS solution at pH 7.0. Interestingly, it is observed that after each addition of hydrazine, a rapid increase in current was observed in amperometric measurements. The modified electrode exhibits fast electron exchange behavior as the response time to achieve 95% of the steady-state current was within 3 s. A relationship between the response current and hydrazine concentration for the fabricated sensor is demonstrated in the inset of Fig. 7(a). It exhibits that with increasing the hydrazine concentrations, the response current also increases linearly. The calculated correlation coefficient (R) is estimated to be $R = 0.9906$. Fig. 7(b) shows the calibration curve of

Table 1
Comparison of analytical performances of various electrode-based hydrazine sensors.

Electrode materials	Sensitivity ($\mu A\,cm^{-2}\,(M^{-1})$)	Detection limit (μM)	Response time (s)	Linear range	Ref.
ZnO nanorods	4.76	2.2	<10	0.2–2.0 μM	[16]
SWCNT and catechin hydrate	0.183	2.0	–	0.5 μM–1 mM	[17]
C@ZnO nanorods	9.4	0.1	<4	0.1–3.8 mM	[18]
Carbon nanotube powder	0.9944	NA	<3	NA	[19]
Nano-Au/Ti	1.117	42	–	0–40 mM	[20]
BiHCF-modified CCEs	4.2	3	–	7 μM–1.1 mM	[21]
Nickel hexacyanoferrate	0.26	2.28	<3	1 μM–50 mM	[22]
Carbon nanotube-wired ZnO nanoflower	3.49	0.18	<3	0.1–3.8 mM	[23]
Ru-complex films	–	8.5	–	10 μM–10 mM.	[24]
PEG-coated ZnS NPs	89.3	1.073	<3	1 μM–3 mM	This work

the fabricated amperometric hydrazine sensor. From slope of calibration curve, the sensitivity of P-ZnS NPs based hydrazine sensor has been found to be 89.3 $\mu A\,cm^{-2}\,\mu M^{-1}$. The obtained sensitivity for the fabricated hydrazine sensor is much higher than the other reported hydrazine chemical sensor fabricated based on amperometric principle such as ZnO nanorods [16], SWCNT and catechin hydrate [17], Carbon coated ZnO nanorods [18], carbon nanotube [19], nano-Au/Ti electrode [20], BiHCF-modified CCEs [21], nickel hexacyanoferrate [22], Carbon nanotube wired ZnO nanoflowers [23], Ru-complex films [24] etc. In addition, the calculated detection limit estimated based on signal to noise ratio (S/N), is found to be 1.07 μM. To the best of our knowledge, this is the first report in which P-ZnS NPs were used to modify Au electrode for the fabrication of highly sensitive hydrazine sensor. To exhibit the superiority of the prepared P-ZnS NPs based hydrazine sensor, a comparison of the characteristic and performances of the fabricated sensor with already reported hydrazine sensors has been made based on the utilization of different materials as the working electrode (Table 1). By comparing the performances and characteristics, it is clear that the fabricated P-ZnS NPs based hydrazine sensor exhibits an excellent performance.

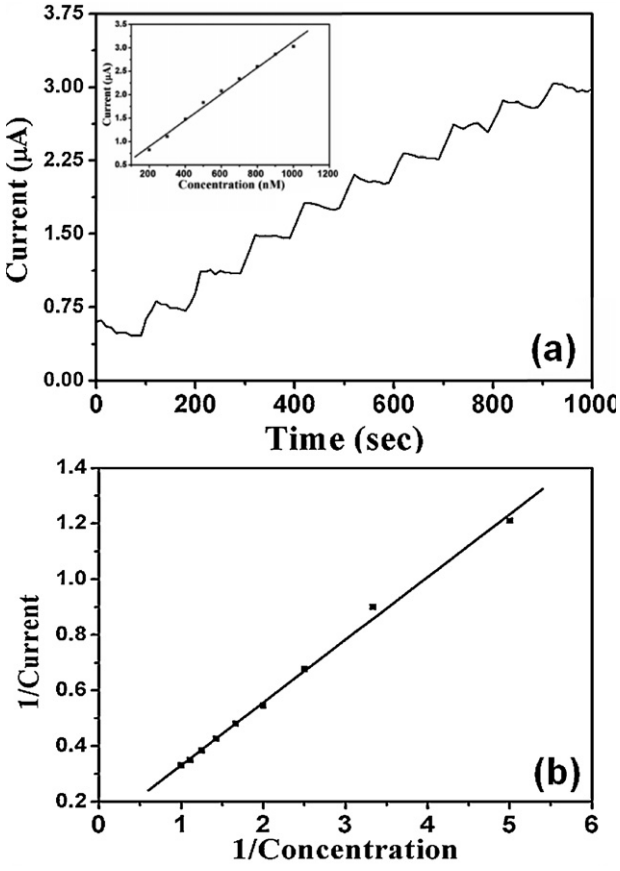

Fig. 7. (a) Amperometric response of the P-ZnS NPs/Au electrode with successive addition of hydrazine into 0.1 M PBS buffer solution (pH 7.0). (b) The plot of 1/Current vs 1/Concentration exhibiting a linear relationship with the steady state current and hydrazine concentration.

4. Conclusions

In summary, a very facile and rapid synthesis method has been developed to produce monodispersed PEG-coated ZnS nanoparticles (P-ZnS NPs). The synthesized P-ZnS NPs exhibits good structural and optical properties. From application point of view, the synthesized nanoparticles have been used as efficient electron mediators for the fabrication of highly sensitive hydrazine chemical sensor. The obtained sensitivity and detection limit for the fabricated hydrazine chemical sensor have been found to be ~89.3 $\mu A\,cm^{-2}$ μM and 1.07 μM, respectively. To the best of our knowledge, this is the first report in which a very high sensitivity and low-detection limit have been observed for the hydrazine sensor fabricated based on P-ZnS NPs. By this work, it could be concluded that P-ZnS NPs can be used for the fabrication of highly sensitive hydrazine sensor with fast response time and low-detection limit.

Acknowledgements

SKM and Khushboo are thankful to Department of Science and Technology (DST) and Council of Scientific & Industrial Research (*CSIR*), India for the financial assistance and fellowships. AU is thankful to the Ministry of Higher Education, Kingdom of Saudi Arabia for granting a Collaborative Research Centre on Sensors and Electronic Devices to Najran University, Saudi Arabia on dated 24/3/1432 H, 27/02/2011.

References

[1] H.S. Nalwa (Ed.), Encyclopedia of Semiconductor Nanotechnology, American Scientific Publishers, Los Angeles, USA, 2011.
[2] Y. Lin, H.S. Nalwa (Eds.), Handbook of Electrochemical Nanotechnology, American Scientific Publishers, Los Angeles, USA, 2009.
[3] A. Umar, Y.B. Hahn (Eds.), Metal Oxide Nanostructures and Their Applications, American Scientific Publishers, Los Angeles, USA, 2010.
[4] S. Garrod, M.E. Bollard, A.W. Nicholls, S.C. Connor, J. Connelly, J.K. Nicholson, E. Holmes, Chem. Res. Toxicol. 18 (2005) 115.
[5] G.E. Collins, Actuators Sensors B B35 (1996) 202.
[6] C. Gojon, B. Dureault, N. Hovnanian, C. Guizard, Actuators Sensors B. B38 (1997) 154.
[7] D.L. Ellis, M.R. Zakin, L.S. Bernstein, M.F. Rubner, Anal. Chem. 68 (1996) 817.
[8] X.S. Fang, C.H. Ye, L.D. Zhang, Y.H. Wang, Y.C. Wu, Adv. Funct. Mater. 15 (2005) 63.
[9] D. Moore, Z.L. Wang, J. Mater. Chem. 16 (2006) 3898.
[10] H. Zhang, L. Qi, Nanotechnology 17 (2006) 3984.
[11] D. Moore, Y. Ding, Z.L. Wang, Angew. Chem. Int. Ed. 45 (2006) 5150.
[12] (a) Z. Wang, L.L. Daemen, Y. Zhao, C.S. Zha, R.T. Downs, X. Wang, Z.L. Wang, R.J. Hemley, Nat. Mater. 4 (2005) 922;
(b) D. Kim, P. Shimpi, P.X. Gao, Sci. Adv. Mater. 2 (2010) 421.

[13] (a) I.A. Banerjee, L. Yu, H. Matsui, J. Am. Chem. Soc. 127 (2005) 16002;
(b) X. Ma, Z. Yu, J. Song, Sci. Adv. Mater. 2 (2010) 219.
[14] (a) J.S. Hu, L.L. Ren, Y.G. Guo, H.P. Liang, A.M. Cao, L.J. Wan, C.L. Bai, Angew. Chem. Int. Ed. 44 (2005) 1269;
(b) X. Xu, X. Fang, H. Zeng, T. Zhai, Y. Bando, D. Golberg, Sci. Adv. Mater. 2 (2010) 273.
[15] A. Umar, M.M. Rahman, S.H. Kim, Y.B. Hahn, Chem. Commun. (2008) 166.
[16] A. Umar, M.M. Rahman, S.H. Kim, Y.B. Hahn, J. Nanosci. Nanotechnol. 8 (2008) 3216.
[17] Y.H. Ni, J.S. Zhu, L. Zhang, J.M. Hong, Cryst Eng. Commun. (2010), doi:10.1039/b923857n.
[18] J. Liu, Y. Li, J. Jiang, X. Huang, Dalton Trans. 39 (2010) 8693.
[19] Y.D. Zhao, W.D. Zhang, H. Chen, Q.M. Luo, Talanta 58 (2002) 529.
[20] Q. Yi, W. Yu, W. Wang, J. Anal. Chem. 633 (2009) 159.
[21] J.B. Zheng, Q.L. Sheng, L. Li, Y. Shen, J. Electroanal. Chem. 611 (2007) 155.
[22] A. Salimi, K. Abdi, Talanta 63 (2004) 475.
[23] B. Fang, C.H. Zhang, W. Zhang, G.F. Wang, Electrochim. Acta. 55 (2009) 178.
[24] J.S. Pinter, K.L. Brown, P.A. DeYoung, G.F. Peaslee, Talanta 71 (2007) 1219.